# An Unified Approach for Calculation of Movement–Induced Fluid Loads in Channel Networks

Ronald Beck, Jürgen Stabel, Mingmin Ren

Framatome ANP GmbH, Erlangen, Germany

## ABSTRACT

Many problems of fluid–structure interaction in reactor technology are governed by channel like fluid domains, for instance the analysis of fuel storage racks under seismic load or the assesment of the dynamical behaviour of fuel rods under cross and axial flow. In both cases it is possible to simulate the fluid domain as a network of plane flow channels. However, the underlying physical mechanisms are very different on account of the main flow. In this paper an unified calculation method for channel networks is developed. It provides very efficiently movement–induced fluid loads based on the current gap configuration. Large changes of the gap width are allowed.

The method originates from an assumption about the velocity distribution of a plane, incompressible, laminar viscous flow in a single channel. This distribution depends on the gap width, the wall velocity and the flow rate. The flow rate may be produced by an adjacent channel. From the known velocity distribution in a single channel follows the pressure field in a single channel by integration of the pressure equation, a Poisson equation with Neumann boundary condition. The Neumann boundary condition contains a partial time derivative of the velocity distribution. Consequently the pressure field depends on the gap width, the wall velocity and acceleration as well as the flow rate and its first time derivative.

The channels are coupled by the Nodal and Mesh Rules which state the balance of mass and pressure difference respectively. A differential–algebraic system of index 1 for the flow rate is obtained. From this differential–algebraic system follows a dynamical system by time differentiation of the nodal equations. The mesh relations are unchanged. Finally the dynamical system for the flow rate and the structural equation are simultaneously solved.

## INTRODUCTION

The flow domain of numerous fluid coupled structural vibration problems can be considered as a network of channels. An obvious example is the analysis of fuel storage racks under seismic load. Up to 20 racks stand freely in a pool with stagnant water, separated only by very small water gaps. Typical dimensions of a rack are 3m x 2m x 4.5m (length x width x height). The smallest water gap is about 10mm. During an earthquake the fluid motion highly influences the structure motion and vice versa which becomes a strong interaction. This interaction must be considered for the whole pool with all racks included, not only for a single rack [10]. The relevant fluid forces are called movement–induced [5]. They only appear if a Galilei–invariant structure motion exists. Fig. 1a) shows schematically the top view of a wet storage with fuel storage racks. The movement–induced flow shall be plane. It is then possible to imagine the flow domain as coupling of channels. The resulting network is shown in Fig. 1b). To take into account the important vertical flow [6], a neutral plane hypothesis [6] together with a correction factor [1] may be used. The cited correction factor arises from an analytical work.

Fig. 1: Wet storage with fuel storage racks; a) schematic top view, b) resulting network

A not so obvious example is the assesment of the dynamical behaviour of fuel rods under cross and axial flow. In this case the modelling as a channel network is more abstract. Up to now, we have performed no such calculation.

Both examples essentially differ from each other in the existence of a main flow. Such a main flow can lead to some interesting phenomena, for instance the fluid–elastic instability, which are not possible in a stagnant fluid. However, the channel technique is uniformly developed.

The basic idea of a channel network is not new. It has been previously presented in Sharp, Wenzel [9]. Tab. 1 summarizes the extensions.

Tab. 1: Comparsion of both channel techniques

| | Sharp, Wenzel | Beck, Stabel, Ren |
|---|---|---|
| Dimension of flow | 1 | 2 |
| Type of flow | frictionless | laminar viscous and limited turbulent |
| | stagnant | stagnant and with main flow |
| | closed | closed and open |
| Number of bodies | several | several |
| Allowed changes of gap width | small | large |
| Result of computation | added mass matrix | fluid force including inertial, damping, stiffness and dynamic buoyancy effect |
| | for a fixed gap configuration | for the current gap configuration |
| Character of channel flow rate | structural constrained variable | dynamical variable |

## CHANNEL TECHNIQUE

The development of the channel technique consists of two steps. In the first step a single channel is considered. For this channel an assumption about the velocity distribution is made. Such an assumption is common practice [8], [11]. In contrary to the cited literature, the flow shall be laminar viscous. It shall also be plane and incompressible. From a known velocity field, the corresponding pressure field is obtained by solving the pressure equation, a Poisson equation with Neumann boundary condition [2]. This holds for an incompressible laminar viscous flow. Here the solving is performed analytic–approximately by means of the least square method [4]. The velocity distribution depends on the gap width, the wall velocity and the flow rate. The flow rate is caused by adjacent channels in the sense of squeezing through. It is determined by channel coupling. Due to the Neumann boundary condition, the first time derivative of these quantities enters the pressure distribution. Consequently the pressure distribution depends on the gap width, the wall velocity and acceleration as well as the flow rate and its first time derivative.

In the second step the single channels must be coupled. A hydraulic network, such as the channel network at hand, is governed by the Nodal and Mesh Rules. These rules state the balance of mass and pressure difference respectively. The pressure difference includes both the reversible and irreversible components. From the Nodal Rule follows a system of nodal equations which contain only the channel flow rate but not its first time derivative. From the Mesh Rule follows a system of mesh equations which contain both the channel flow rate and its first time derivative. The sum of the nodal and mesh equations forms a differential–algebraic system of index 1 for the unknown flow rate. A system of differential equations is simpler to solve than a system of differential–algebraic equations. Therefore the nodal equations are differentiated with respect to time. The time differentiated nodal equations and the unchanged mesh equations form an implicit differential equation system for the unknown flow rate.

In the time differentiation an information loss occurs. Therefore, an arbitrary choice of the initial condition for the unknown flow rate violates the Nodal Rule. The choice must be accomplished while maintaining mass consistency. Finally, the dynamical systems for the unknown flow rate (semidiscrete fluid equation) and the generalized structural displacement as well as velocity (semidiscrete structure equation) are simultaneously integrated on a mass consistent manifold of the phase space.

**Single Channel**

Fig. 2a) shows a single channel with a width of 2h and a length of 2L. The left wall is indicated by l, the right wall by r, the upper channel end by o and the lower channel end by u. These letters will occur as indices in the following. Furthermore it is advantageously to use both an inertial frame of reference $\Sigma$ with inherent cartesian coordinates x,y and a noninertial frame of reference $\Sigma'$ with inherent cartesian coordinates $x', y'$. In the first frame all physical quantities are measured but in the second frame they are localized. The continuity and pressure equations must be adjusted appropriately after which the formulation is straight forward, for instance the formulation of boundary conditions.

Fig. 2b) shows the corresponding directed branch. It contains the entire topological information. In the presented direction illustrated by the arrow, the left channel wall lies on the left side of the directed branch and the right wall on the right side, the upper channel end corresponds with the upper node of the directed branch and the lower end with the lower node. The same holds for the x– and y–direction. All lines in Fig. 1b) can be replaced by such directed branches.

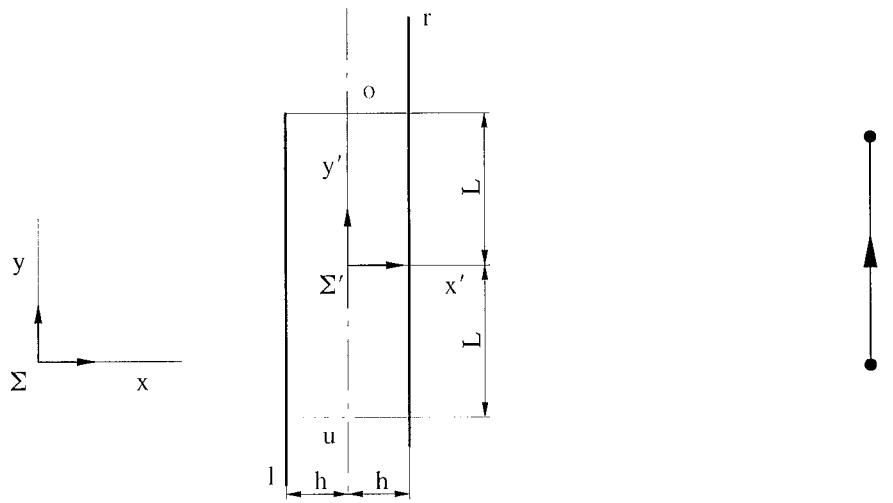


Fig. 2: Single channel; a) geometry and frame of reference, b) directed branch

The channel ratio $\tau$ is introduced as $\tau = h/L$. For $\tau \leq 0.1$, a slender channel, the velocity distribution is assumed to be

$$u = -\frac{1}{4}\left(3\,(x'/h) - (x'/h)^3\right)\left(\dot{x}_l - \dot{x}_r\right) + \frac{1}{2}\left(\dot{x}_l + \dot{x}_r\right), \tag{1}$$

$$v = -\left(1 - (x'/h)^2\right)\alpha - \frac{1}{2}\,(x'/h)\left(\dot{y}_l - \dot{y}_r\right) + \frac{1}{2}\left(\dot{y}_l + \dot{y}_r\right) + \frac{3}{4\tau}\left(1 - (x'/h)^2\right)(y'/L)\left(\dot{x}_l - \dot{x}_r\right) \tag{2}$$

with u and v – fluid velocity in x– and y–direction, $\dot{x}_l$ and $\dot{x}_r$ – velocity of the left and right wall in x–direction, $\dot{y}_l$ and $\dot{y}_r$ – velocity of the left and right wall in y–direction, $\alpha$ – flow rate like quantity. This distribution fulfils the continuity equation in the fluid domain as well as the no–slip condition at the walls. It contains the special cases of a Poiseuille and Couette flow.

The velocity distribution leads to a pressure distribution as previously described. Finally, the pressure $p_u$ in the point $(0, -L)_{x',y'}$ follows as

$$p_u = g_1(\varrho, L, \tau)\left(\ddot{x}_l - \ddot{x}_r\right) + g_2(\varrho, L, \tau)\left(\ddot{y}_l + \ddot{y}_r\right) + g_3(\mu, L, \tau)\left(\dot{x}_l - \dot{x}_r\right)$$

$$+ g_4(\varrho, L, \tau)\,\dot{\alpha} + g_5(\mu, L, \tau)\,\alpha + g_6(\varrho, \tau)\left(\dot{x}_l - \dot{x}_r\right)^2 + g_7(\varrho, \tau)\left(\dot{x}_l - \dot{x}_r\right)\alpha + \beta, \tag{3}$$

the pressure $p_o$ in the point $(0, L)_{x',y'}$ as

$$p_o = g_1(\varrho, L, \tau)\left(\ddot{x}_l - \ddot{x}_r\right) - g_2(\varrho, L, \tau)\left(\ddot{y}_l + \ddot{y}_r\right) + g_3(\mu, L, \tau)\left(\dot{x}_l - \dot{x}_r\right)$$
$$- g_4(\varrho, L, \tau)\,\dot{\alpha} - g_5(\mu, L, \tau)\,\alpha + g_6(\varrho, \tau)\left(\dot{x}_l - \dot{x}_r\right)^2 - g_7(\varrho, \tau)\left(\dot{x}_l - \dot{x}_r\right)\alpha + \beta\ , \qquad (4)$$

the force $f_{xl}$ per unit depth acting at the left wall in x–direction as

$$f_{xl} = g_8(\varrho, L, \tau)\left(\ddot{x}_l - \ddot{x}_r\right) + g_9(\varrho, L, \tau)\,\ddot{x}_r + g_{10}(\mu, \tau)\left(\dot{x}_l - \dot{x}_r\right) + g_{11}(\varrho, L, \tau)\left(\dot{x}_l - \dot{x}_r\right)^2 - 2L\beta\ , \qquad (5)$$

the force $f_{yl}$ per unit depth acting at the left wall in y–direction as

$$f_{yl} = -\frac{\mu}{\tau}\left(\dot{y}_l - \dot{y}_r\right) - \frac{4\mu}{\tau}\,\alpha\ , \qquad (6)$$

the force $f_{xr}$ per unit depth acting at the right wall in x–direction as

$$f_{xr} = -g_8(\varrho, L, \tau)\left(\ddot{x}_l - \ddot{x}_r\right) + g_9(\varrho, L, \tau)\,\ddot{x}_l - g_{10}(\mu, \tau)\left(\dot{x}_l - \dot{x}_r\right) - g_{11}(\varrho, L, \tau)\left(\dot{x}_l - \dot{x}_r\right)^2 + 2L\beta \qquad (7)$$

and the force $f_{yr}$ per unit depth acting at the right wall in y–direction as

$$f_{yr} = \frac{\mu}{\tau}\left(\dot{y}_l - \dot{y}_r\right) - \frac{4\mu}{\tau}\,\alpha \qquad (8)$$

with $g_1 ... g_{11}$ – singular functions in $\tau$ of order 0 to 3 for $\tau \to 0$, $\beta$ – pressure in the point $(0, 0)_{x',y'}$, $\varrho$ – density, $\mu$ – dynamic viscosity. The forces have been calculated considering the Navier–Poisson Law of a Newtonian Fluid [3].

Tab. 2 summarizes the physical meaning of the terms in Eq. (1) through (8).

Tab. 2: Physical meaning of the terms in Eq. (1) through (8)

| velocity | | pressure | | force | |
|---|---|---|---|---|---|
| 1 / 1 | squeezing | 3 / 1 | inertia by squeezing | 5 / 1 | inertia by squeezing |
| 1 / 2 | rigidly moving | 3 / 2 | inertia by dragging | 5 / 2 | inertia by absolute motion |
| 2 / 1 | flowing through | 3 / 3 | damping by squeezing | 5 / 3 | damping by squeezing |
| 2 / 2 | dragging | 3 / 4 | inertia by flowing through | 5 / 4 | build–up by squeezing |
| 2 / 3 | dragging | 3 / 5 | damping by flowing through | 5 / 5 | absolute value |
| 2 / 4 | squeezing | 3 / 6 | build–up by squeezing | 6 / 1 | damping by dragging |
| | | 3 / 7 | build–up by squeezing and flowing through | 6 / 2 | damping by flowing through |
| | | 3 / 8 | absolute value | | |

Column 1, 3, 5: equation / term

**Network Of Channels**

The channel coupling is described by means of an example. Considered are two cuboids in a water pool with one prescribed inflow and two prescribed outflows (Fig. 3a). The inflow and outflows may be transient. Fig. 3b) shows the corresponding graph. It consists of 10 directed branches and 6 nodes. There exist 10 flow rates, 3 are prescribed

and 7 are unknown. There also exist 7 linear independent equations, 5 time differentiated nodal and 2 mesh equations. Therefore the problem is fully defined.


Fig. 3: Two cuboids in a water pool; a) schematic top view, b) corresponding graph

It holds

$$d\dot{m}_{6o}/dt - d\dot{m}_{1u}/dt = 0 \tag{9}$$

for the 1st node with $\dot{m}_{6o}$ – mass flow in the 6th channel at the upper end (unknown) and $\dot{m}_{1u}$ – mass flow in the 1st channel at the lower end (unknown), t – time,

$$d\dot{m}_{1o}/dt - d\dot{m}_{7u}/dt - d\dot{m}_{2u}/dt = 0 \tag{10}$$

for the 2nd node with $\dot{m}_{1o}$ – mass flow in the 1st channel at the upper end (unknown), $\dot{m}_{7u}$ – mass flow in the 7th channel at the lower end (unknown) and $\dot{m}_{2u}$ – mass flow in the 2nd channel at the lower end (unknown),

$$d\dot{m}_{2o}/dt - d\dot{m}_{3u}/dt - d\dot{m}_{9}/dt = 0 \tag{11}$$

for the 3rd node with $\dot{m}_{2o}$ – mass flow in the 2nd channel at the upper end (unknown), $\dot{m}_{3u}$ – mass flow in the 3rd channel at the lower end (unknown) and $\dot{m}_{9}$ – mass flow in the 9th channel (known),

$$d\dot{m}_{3o}/dt - d\dot{m}_{10}/dt - d\dot{m}_{4u}/dt = 0 \tag{12}$$

for the 4th node with $\dot{m}_{3o}$ – mass flow in the 3rd channel at the upper end (unknown), $\dot{m}_{10}$ – mass flow in the 10th channel (known) and $\dot{m}_{4u}$ – mass flow in the 4th channel at the lower end (unknown),

$$d\dot{m}_{4o}/dt + d\dot{m}_{7o}/dt - d\dot{m}_{5u}/dt = 0 \tag{13}$$

for the 5th node with $\dot{m}_{4o}$ – mass flow in the 4th channel at the upper end (unknown), $\dot{m}_{7o}$ – mass flow in the 7th channel at the upper end (unknown) and $\dot{m}_{5u}$ – mass flow in the 5th channel at the lower end (unknown),

$$\Delta_+p_1 + \Delta_+p_7 + \Delta_+p_5 + \Delta_+p_6 = 0 \tag{14}$$

for the ①⑦⑤⑥ mesh with $\Delta_+p_1$ – pressure difference $(p_o - p_u)$ between the upper and lower end of the 1st channel including built–up pressure and pressure loss arising from channel coupling, $\Delta_+p_7$, $\Delta_+p_5$, $\Delta_+p_6$ – analogous meaning,

$$\Delta_+p_2 + \Delta_+p_3 + \Delta_+p_4 - \Delta_+p_7 = 0 \tag{15}$$

for the ②③④⑦ mesh with $\Delta_+p_2$ – pressure difference $(p_o - p_u)$ between the upper and lower end of the 2nd channel including built–up pressure and pressure loss arising from channel coupling, $\Delta_+p_3$, $\Delta_+p_4$, $\Delta_+p_7$ – analogous

meaning.

This procedure was formalized for the general case.

**Verification**

In the initial verification, two models are analysed. These two models are one and four cuboids in a water pool respectively (Tab. 3). The cuboids are excited by a prescribed time history of pool displacement. Comparsions use experimental data (one cuboid, [8]) and results based on potential theory as well as CFD simulation (four cuboids, [7]). These two models verify the case of a stagnant fluid. The case of a superimposed main flow will be subsequently verified.

Tab. 3: Cuboids in a water pool

| | One cuboid | Four cuboids |
|---|---|---|
| | 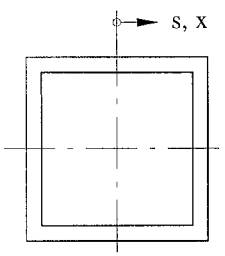  | 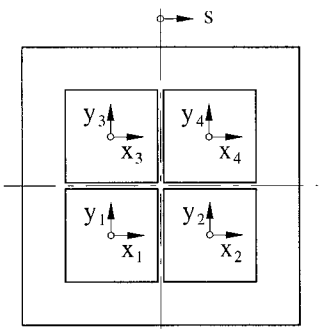  |
| Structur | | |
| Cuboid dimensions | □101.6mm x 203.2mm | □2300mm x 30mm |
| Cuboid mass | 6.8kg | 3200kg |
| Gap width cuboid – pool wall<br>Gap width cuboid – cuboid | 12.7mm<br>— | 600mm<br>30mm |
| Spring cuboid – pool<br>Spring cuboid – cuboid | anisotropic<br>— | isotropic<br>none |
| Degree of freedom | 1; x | 8; $x_1$,$y_1$, ..., $x_4$,$y_4$ |
| Fluid | | |
| Kind | water | |
| Flow characteristic | plane, incompressible | |
| Excitation | | |
| Kind | prescribed harmonic motion s of the pool with | |
| | unknown amplitude | 10mm amplitude |

The one cuboid example goes back to the experimental work of Radke [8]. Radke measured for several excitation frequencies $f_{err}$ the acceleration amplitude $\hat{\ddot{s}}$ of the pool as well as the acceleration amplitude $\hat{\ddot{x}}$ of the cuboid and formed the ratio $\hat{\ddot{x}}/\hat{\ddot{s}}$ (Fig. 4). No information could be found regarding the excitation amplitude $\hat{s}$ in [8]. It was therefore necessary to calculate the ratio $\hat{\ddot{x}}/\hat{\ddot{s}}$ for two extreme cases: $\hat{s}$ = 0.5mm and $\hat{s}$ = 6.0mm (Fig. 4). In the first case a relative motion cuboid–pool up to 2.16mm was obtained and in the second up to 9.89mm. The original gap was 12.7mm. Fig. 4 shows a good agreement between the results from the experiment and the channel technique over the entire frequency interval for the larger excitation amplitude. However, for the smaller excitation amplitude the good agreement holds only outside the resonance.

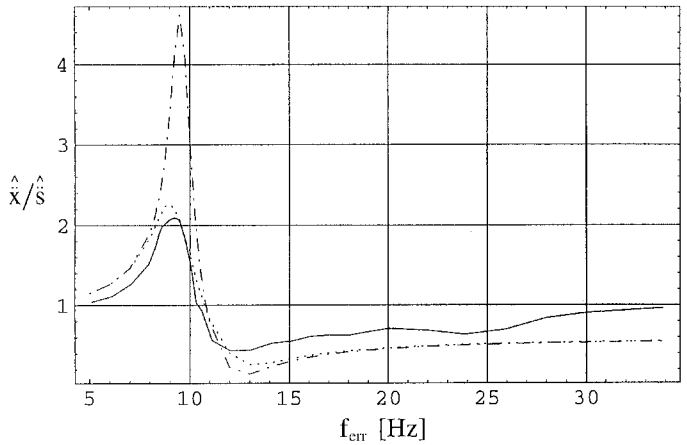


_____ experiment, _ _ _ channel technique with $\hat{s} = 0.5$mm, ..... channel technique with $\hat{s} = 6.0$mm

Fig. 4: One cuboid in a water pool, comparsion of results

The four cuboid example goes back to a numerical work by Ren, Stabel and Hinderks [7]. They compare in [7] a potential theory of second order with a CFD simulation (STAR code) for one excitation frequency. The cited work was extended by the potential theory of first order. By means of this theory it can be shown, that only 6 different eigenfrequencies exist and that only 2 of them are excited (Fig. 5). Both effects arise from the multiple symmetry in the problem: four identical cuboids with identical isotropic supports as well as a double symmetric fluid domain. It holds (Fig. 5):

$$x_1 = x_2 = x_3 = x_4 = x \quad , \quad y_1 = -y_2 = -y_3 = y_4 = -y \quad . \tag{16}$$

Both quantities x and y describe the cuboid motion entirely.

3.13Hz 3.63Hz

Fig. 5: Four cuboids in a water pool, excited eigenforms

The pool is harmonically moved in s–direction with a frequency $f_{err}$. For several frequencies the resulting amplitudes $\hat{x}$ and $\hat{y}$ are calculated using the potential theory of first order and the channel technique (Fig. 6). Fig. 6 also contains the results from [7]. There exists a good agreement between the amplitudes $\hat{x}$. Greater differences appear however for the amplitudes $\hat{y}$. The potential theory of first order overestimates these amplitudes: $2 \cdot 13.5\text{mm} = 27\text{mm}$ (original gap: 30mm). The channel technique seems to be more realistic: $2 \cdot 3\text{mm} = 6\text{mm}$.

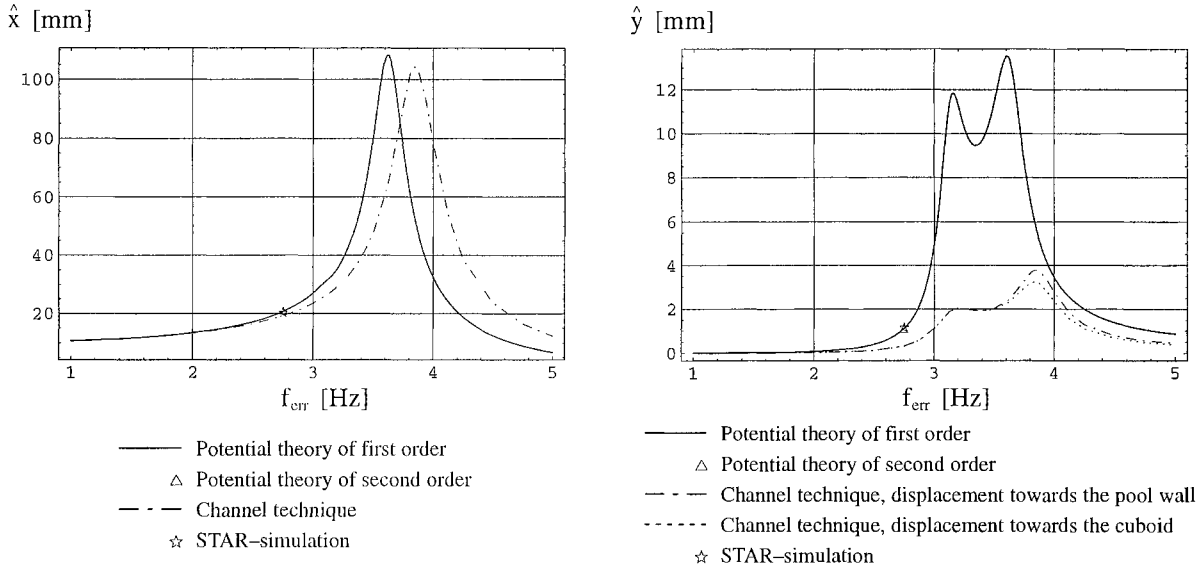


Fig. 6: Four cuboids in a water pool, comparsion of results

## SUMMARY

The developed channel technique provides very efficiently movement–induced fluid loads based on the current gap configuration. Large changes of the gap width are allowed. In the initial verification, two models for a stagnant fluid was analysed.

## REFERENCES


1. Kiss, E., "Analysis of the Fundamental Vibration Frequency of a Radial Vane Internal Steam Separator Structure", *Proceedings of Conference on Flow–Induced Vibrations in Reactor System Components*, ANL–7685, pp. 335–343, Argonne National Laboratory, Argonne III, May 1970.
2. Landau, L. D., Lifschitz, E. M., *Lehrbuch der Theoretischen Physik, Band VI, Hydrodynamik*, Akademie Verlag, Berlin, 1991.
3. Malvern, L. E., *Introduction to the Mechanics of a Continuous Medium*, Prentice–Hall, Englewood Cliffs, N. J., 1969.
4. Michlin, S. G., *Variationsmethoden der mathematischen Physik*, Akademie–Verlag, Berlin, 1962.
5. Naudascher, E., Rockwell, D., *Flow–Induced Vibration, An Engineering Guide*, A. A. Balkema, Rotterdam, 1994.
6. Ren, M., Stabel, J., "Comparsion of Different Analytical Formulations for FSI between Fuel Storage Racks", *Transactions of the 15th International Conference on Structural Mechanics in Reactor Technology*, Vol. VII, pp. 87–94, Seoul, Korea, August 1999.
7. Ren, M., Stabel, J., Hinderks, M., "Validation of Fluid–Structure–Interaction Formulation Used in Fuel Storage Multi–Rack Dynamic Model", ASME PVP–402–1, pp. 73–79, 2000.
8. Scavuzzo, R. J., Stokey, W. F., Radke, E. F., "Dynamic Fluid–Structure Coupling of Rectangular Modules in Rectangular Pools", ASME PVP–39, pp. 77–85, June 1979.
9. Sharp, G. R., Wenzel, W. A., "Hydrodynamic Mass Matrix for a Multibodied System", *Journal of Engineering for Industry*, 1974, pp. 611–618.
10. Singh, K. P., Soler, A. I., "Chin Shan Analyses Show Advantages of Whole Pool Multi–Rack Approach", *Nuclear Engineering International*, March 1991, pp. 37–40.
11. Soler, A. I., Singh, K. P., "Dynamic Coupling in a Closely Spaced Two–Body System Vibrating in a Liquid Medium: The Case of Fuel Racks", *The 3rd Keswick International Conference in Nuclear Plants*, pp. 815–834, Keswick, U.K., May 1982.